Supplementary Information

Energy transfer in near-infrared photoluminescent PbS/CdS quantum dot-based three-dimensional networks and films

*Denis Pluta, Rebecca T. Graf, Dirk Dorfs, Nadja C. Bigall**

Experimental Section and Methods

Chemicals

Lead oxide (PbO, 99.99 %) and cadmium oxide (CdO, 99.998 %) were purchased from alfa aesar. Oleic acid (OA, 90 %) was purchased from ABCR. Toluene (puris p.a.) was purchased from Merck. Octadecene (ODE, 90 %), hexamethyldisilane ($(TMS)_2S$, 98 %), methanol (MeOH, 99.8 %), hexane (p.a), tetrachloroethylene (TCE, >99.9 %), diphenyl ether (DPE, 99 %), 11-mercaptoundeconoic acid (MUA, 95 %), 3-mercaptopropionic acid (MPA, 99 %), acetone (99.8 %), potassium hydroxide (KOH, 85 %), chloroform (99 %), yttrium chloride hexahydrate (YCl3 · 6 H2O, 99.99%) and (3-mercaptopropyl)trimethoxysilane (MPTMS, 95 %) were purchased from Sigma-Aldrich. Nitric acid (HNO3, >69 %) and hydrochloric acid (HCl, ≥37 %) were purchased from Honeywell.
All chemicals were used without further purification.

Synthesis of PbS QDs:

The synthesis of the PbS QDs was adapted from literature from Zhang et al.[1] For the synthesis of 3.7 nm PbS QDs [4.7 nm PbS QDs] 1.35 g [1.35 g] PbO (6.1 mmol), 27 mL [47.1 mL] oleic acid (85.5 mmol [149.2 mmol]) and 43.1 mL [43.1 mL] ODE (134.7 mmol) were degassed in a 100 mL flask at 110 °C for 30 min, using a Schlenk line. The flask was filled with nitrogen, heated to 95 °C and after removing the heating mantle 630 µL [630 µL] (3.0 mmol) $(TMS)_2S$ dissolved in 5 mL [5 mL] ODE were injected. The reaction mixture was cooled to 30 °C and the PbS QDs were precipitated with methanol, redispersed in hexane and centrifuged at 10621 rcf a total of two times. After dispersing the QDs in 7 mL TCE, the lead concentration was determined with atomic absorption spectrometry (AAS).

Synthesis of PbS/CdS QDs:

The CdS shell was introduced to the previously synthesized PbS QDs with a cation exchange approach, adapted from Zhao et al.[2] 2.06 g CdO (16 mmol), 12.3 mL oleic acid (38.8 mmol)

and 32.8 mL DPE (206.1 mmol) were loaded in a 100 mL flask and the temperature was raised to 255 °C under a nitrogen atmosphere. After cooling to room temperature, the solution was degassed at 100 °C for 10 min under vacuum and reopened to nitrogen. 50 mL of dry toluene was added and the solution was heated to 100 °C. 0.6 mmol of the previously synthesized PbS QDs were precipitated with methanol and redispersed in 3 mL dry toluene and injected into the flask. (The necessary volume was calculated with the determined lead concentration from the AAS measurement) After 30 min at 100 °C the solution was allowed to cool to room temperature and the PbS/CdS QDs were precipitated with methanol and dispersed in hexane twice after finally being dispersed in 4 mL TCE. The lead concentration was determined *via* AAS.

Ligand exchange:

The ligand exchange of the PbS/CdS QDs was adapted from literature from Kodanek et al.[3], which is based on a procedure from Bagaria et al.[4] Here, 1.5 mL of the PbS/CdS QDs with a lead concentration of 12.45 g L^{-1} were precipitated with methanol and redispersed in 560 µL of hexane. Afterwards, the QD dispersion was added to a mixture of 29 mg KOH, 90 mg MUA or 33.7 µL MPA and 1.39 mL methanol. After 2 h on an orbital shaker and centrifugation, the QDs were redispersed in 560 µL 0.01 M aqueous KOH. The QDs were cleaned with a centrifuge filter (100.000 MWCO) by diluting the dispersion to a total volume of roughly 10 mL and centrifugation until roughly 9 mL of the solvent passed through the filter. The concentrated dispersion was diluted to 10 mL again and the filtration was repeated a total of three times. The lead concentration of the final concentrated QD dispersion was determined *via* AAS.

Synthesis of hydrogels:

The preparation of the three-dimensional networks is based on a method from Zámbó et al.[5] and has been described in a previous work.[6] 400 µL of the PbS/CdS QD colloidal dispersion in 0.01 M KOH with a lead concentration of 6.636 g L^{-1} was mixed with 50 µL of a 75 mM aqueous $YCl_3 \cdot 6\ H_2O$ solution in a 2 mL centrifugation tube. After homogenization with a vortex, the samples were stored at room temperature. After 16 h additional 50 µL of a 75 mM aqueous $YCl_3 \cdot 6\ H_2O$ solution was added and complete gelation was observed after another 24 h. Afterwards, the supernatant was exchanged a total of 10 times with fresh distilled water in the span of two days, yielding washed hydrogels.

Synthesis of aerogels:

The supernatant of the washed hydrogels were exchanged to acetone by first using water-acetone mixtures (7:1, 4:1, 1:1 and 1:4 water:acetone volume ratios) twice a day (about 7 h apart) and two times per mixture and then pure anhydrous acetone. After exchanging the supernatant 10 times with fresh anhydrous acetone within 5 days (twice a day, about 7 h apart), the solvogels were dried in a critical point dryer (Quorum Technologies, E3100). The gels in the centrifugation tubes were placed in the critical point dryer and after sealing the apparatus, the acetone was replaced with liquid CO_2 by flushing with CO_2 and draining the acetone. After several minutes of flushing, the samples were stored in liquid CO_2 overnight and the flushing step was repeated the next day. Finally, the apparatus was sealed and the temperature was raised to 36 °C, bringing the CO_2 to supercritical conditions (supercritical point: 31.1 °C and 73.9 bar). After reducing the pressure and temperature to ambient conditions, the aerogels were removed from the apparatus and place in a nitrogen filled glovebox.

Functionalization of ITO slides:

ITO-glass slides were used as substrates for the QD film assemblies. In order to increase the adhesion, the slides were functionalized with MPTMS following a procedure from literature.[7] After cleaning the slides with H_2O_2, NH_3 and H_2O at 70 °C for 2 h in a volume ratio of 1:1:5, the slides were rinsed with distilled water and dried. A 1 vol% solution of MPTMS in toluene was prepared (600 µL MPTMS in 60 mL toluene) and the slides were placed inside for 2 h at 50 °C under stirring. They were finally rinsed with toluene, dried and place in a nitrogen filled glovebox for storage.

Preparation of PbS/CdS QD films:

The PbS/CdS QD film assemblies were prepared on functionalized ITO-glass slides. A mold made from scotch tape with a hole with a diameter of 6 mm was placed on the slides and a total amount of 23 µL of the colloidal aqueous QD dispersion with a lead concentration of 6.636 g L^{-1} was added to the mold. The slides were left to dry at ambient conditions over night and placed in a nitrogen filled glovebox for storage.

Spectroscopy:

The colloidal samples were prepared by dispersing them in TCE and filling them in 3 mL quartz cuvettes (10 mm path length), while the aerogels were filled in teflon holders. The absorbance spectra of the colloids were measured with a Cary 5000 UV-Vis-NIR from Agilent

Technologies. The PL, PLQY and PL decay was measured with an Edinburgh instruments FLS 1000, equipped with a liquid N_2 cooled NIR-PMT InGaAs detector for NIR PL measurements and a 980-PMT detector for UV-Vis PL measurements. For the PL decays a EPL 450 pulsed laser, operated at 445.1 nm was used for the excitation in multi-channel scaling (MCS) mode with a repetition rate of 50 kHz. The emission bandwidth was set to 18.9 nm and each sample was measured at five positions of their emission peak as specified in the figures. For the PLQY measurements an integrating sphere from Edinburgh instruments was used.
The PL decays were background corrected and normalized within the measurement software Fluoracle from Edinburgh instruments and then fitted mono- or bi-exponentially within the analysis software FAST, also supplied by Edinburgh instruments. The fitting parameters were used to calculate the average amplitude weighted lifetimes using equation (5).

$$<\tau> = A_1\tau_1 + A_2\tau_2 \quad (5)$$

The optical characterization data can be found in table S12 in the SI.

The PL measurements at cryogenic temperatures were performed on the same Edinburgh FLS 1000, equipped with a N_2 cooled NIR-PMT InGaAs detector. The instrument was coupled with an Oxford instruments OptistatCF cryostat cooled with liquid helium, while the sample chamber was flooded with helium gas.

PL spectra correction and fitting:
All PL spectra were converted from wavelength to energy and corrected using the Jacobian transformation following Mooney et al.[8] by multiplying the PL intensities with (hc/E^2). In addition, the PL spectra, that were collected in the cryogenic measurement setup were linewidth corrected by dividing the PL intensities by the frequency to the power of three.[8]
The linewidth corrected spectra were then fitted with 2-3 Gaussian functions using Origin 2020 from OriginLab. The Gaussian fit data can be found in table S1-S11 in the SI.

Electron microscopy:
Transmission electron microscopy was carried out with a FEI Tecnai G2 F20 TMP transmission electron microscope, operated at 200 kV. The samples were prepared on Quantifoil copper grids with carbon films by dropping the colloidal QD solution or dispersed aerogel in acetone onto them. The grids were then cleaned with active charcoal, as described

by Li et al.[9] The grids were placed on active charcoal in a petri dish and after the addition of ethanol, they were dried under ambient conditions.

Atomic absorption spectrometry (AAS):

To determine the lead concentration of the colloidal QDs, AAS was used. 1 mL aqua regia (6 mL concentrated hydrochloric acid and 2 mL concentrated nitric acid) was used to dissolve 70 µL of PbS/CdS QDs or 10 µL of PbS QDs, after the organic solvent was evaporated by heating. The dissolved sample was added to a 50 mL volumetric flask and filled to 50 mL with distilled water. A set of 6 calibration samples with concentrations between 0 and 20 mg L^{-1} were prepared by adding the appropriate amount of 2 g L^{-1} lead standard solution and 1 mL of aqua regia to 50 mL volumetric flasks, which are then filled to 50 mL with distilled water. The extinction values, measured with the AAS were plotted against their known lead concentration and were fitted with a linear function. The fitting parameters were used to calculate the unknown lead concentration of the sample with the measured extinction value. For the measurements a AA140 flame atomic absorption spectrometer from Varian operated with an acetylene air mixture (ratio 3:7) and a wavelength of 217 nm was used.

In Table S1 – S11 the fit data for the Gaussian fits of the emission spectra measured at cryogenic temperatures are shown. Given is the Temperature (T) in K, the position of the peak (x1, x2, x3) including the standard deviation in eV, the full width at half maximum (FWHM1, FWHM2, FWHM3) including the standard deviation in eV and the area of the peak (A1, A2, A3) including the standard deviation.

Table S1. Gaussian fit data of peak 1 of the MPA film.

T / K	x1	Std x1	FWHM1	Std FWHM1	A1	Std A1
295	0.944	0.00253	0.30962	0.00517	9.46E-47	2.98E-48
270	0.96986	0.00179	0.29505	0.00388	6.50E-47	1.90E-48
240	0.94129	0.00145	0.27588	0.00195	1.29E-46	2.31E-48
210	0.91604	0.00158	0.26261	0.00144	1.89E-46	3.05E-48
180	0.91407	0.00139	0.24653	0.00109	2.14E-46	3.23E-48
150	0.91152	0.0014	0.24158	0.00106	1.99E-46	2.98E-48
120	0.90832	0.00139	0.24199	0.0011	1.69E-46	2.37E-48
90	0.90627	0.0015	0.24534	0.00125	1.33E-46	1.93E-48
70	0.91163	0.0015	0.24256	0.00123	1.15E-46	1.73E-48
55	0.90934	0.0017	0.24726	0.00143	1.00E-46	1.64E-48
40	0.91533	0.00169	0.24049	0.00138	9.11E-47	1.58E-48
20	0.91535	0.00189	0.24118	0.00156	7.89E-47	1.52E-48
10	0.91266	0.00177	0.2476	0.00154	7.43E-47	1.26E-48
7	0.91182	0.00186	0.24904	0.00163	7.38E-47	1.30E-48
4.2	0.92329	0.00172	0.23767	0.00137	7.40E-47	1.36E-48

Table S2. Gaussian fit data of peak 2 of the MPA film.

T / K	x2	Std x2	FWHM2	Std FWHM2	A2	Std A2
295	0.9922	2.29E-04	0.1666	9.99E-04	1.59E-46	3.33E-48
270	1.01121	2.29E-04	0.16035	9.58E-04	1.02E-46	2.03E-48
240	0.99843	1.70E-04	0.15258	5.98E-04	2.01E-46	2.45E-48
210	0.98775	1.96E-04	0.14812	6.50E-04	2.44E-46	3.23E-48
180	0.98708	1.85E-04	0.14209	6.24E-04	2.51E-46	3.32E-48
150	0.98876	1.75E-04	0.13914	6.08E-04	2.31E-46	3.00E-48
120	0.99096	1.56E-04	0.13746	5.61E-04	1.99E-46	2.37E-48
90	0.99364	1.54E-04	0.1374	5.64E-04	1.62E-46	1.91E-48
70	0.99631	1.63E-04	0.13673	5.95E-04	1.35E-46	1.71E-48
55	0.99669	1.77E-04	0.13752	6.42E-04	1.22E-46	1.62E-48
40	0.99906	1.83E-04	0.13669	6.68E-04	1.08E-46	1.55E-48
20	1.00076	1.92E-04	0.13725	7.09E-04	9.72E-47	1.49E-48
10	1.00185	1.76E-04	0.1376	6.46E-04	9.21E-47	1.24E-48
7	1.00204	1.81E-04	0.13783	6.64E-04	9.29E-47	1.27E-48
4.2	1.00305	1.95E-04	0.13546	6.99E-04	8.82E-47	1.33E-48

Table S3. Gaussian fit data of peak 1 of the MUA film.

T / K	x1	Std x1	FWHM1	Std FWHM1	A1	Std A1
295	0.98457	9.58E-04	0.2613	0.00204	2.76E-46	7.74E-48
270	0.98132	9.56E-04	0.26078	0.00172	2.74E-46	6.41E-48
240	0.97731	0.001	0.25729	0.00139	2.70E-46	5.43E-48
210	0.96191	0.00124	0.24928	0.00103	3.28E-46	6.04E-48
180	0.95057	1.60E-03	0.24061	0.00103	3.43E-46	7.03E-48
150	0.9377	0.00273	2.33E-01	1.89E-03	3.26E-46	1.05E-47
120	0.92408	0.00567	0.22762	0.00477	2.92E-46	1.86E-47
90	0.93239	0.00288	0.24391	0.00219	3.07E-46	9.75E-48
70	0.92607	0.00312	0.24605	0.00237	2.89E-46	9.71E-48
55	0.92375	0.00339	0.24643	0.00252	2.78E-46	1.01E-47
40	0.92356	0.00333	0.24705	0.00236	2.66E-46	9.61E-48
20	0.92623	0.00278	0.2508	0.00179	2.79E-46	8.50E-48
10	0.92631	0.00277	0.25285	0.00174	2.81E-46	8.48E-48
7	0.92545	0.00258	0.25722	0.00157	2.93E-46	8.10E-48
6	0.93061	0.00229	0.25591	0.0013	3.23E-46	8.47E-48

Table S4. Gaussian fit data of peak 2 of the MUA film.

T / K	x2	Std x2	FWHM2	Std FWHM2	A2	Std A2
295	1.01526	3.44E-04	0.16409	0.00138	2.24E-46	7.90E-48
270	1.01705	2.82E-04	0.16125	0.00105	2.56E-46	6.55E-48
240	1.02021	2.30E-04	0.1574	7.78E-04	3.07E-46	5.54E-48
210	1.01986	2.33E-04	0.1532	7.32E-04	3.75E-46	6.08E-48
180	1.02052	2.21E-04	0.15075	7.29E-04	4.18E-46	6.99E-48
150	1.02023	2.23E-04	0.15109	8.68E-04	4.56E-46	1.03E-47
120	1.01919	3.07E-04	0.15294	0.00125	4.73E-46	1.82E-47
90	1.01379	5.19E-04	0.1512	0.00119	4.06E-46	1.10E-47
70	1.01199	3.89E-04	0.15296	0.00115	4.10E-46	1.05E-47
55	1.01051	3.68E-04	0.15412	0.0012	4.08E-46	1.09E-47
40	1.01E+00	3.68E-04	1.54E-01	1.25E-03	3.85E-46	1.04E-47
20	1.00761	3.82E-04	0.15283	0.00124	3.85E-46	9.47E-48
10	1.00694	3.87E-04	0.15251	0.00126	3.89E-46	9.51E-48
7	1.00536	3.82E-04	0.15216	0.00125	4.02E-46	9.25E-48
6	1.00362	4.46E-04	0.14897	0.00147	3.94E-46	1.01E-47

Table S5. Gaussian fit data of peak 3 of the MUA film.

T / K	x3	Std x3	FWHM3	Std FWHM3	A3	Std A3
90	1.06853	8.82E-04	0.06574	0.00343	1.53E-47	1.99E-48
70	1.07111	6.48E-04	0.05941	0.00251	1.45E-47	1.37E-48
55	1.07218	5.65E-04	0.05787	0.00221	1.52E-47	1.26E-48
40	1.07313	5.07E-04	0.05749	0.00205	1.56E-47	1.22E-48
20	1.07418	4.32E-04	0.05862	0.00184	1.89E-47	1.35E-48
10	1.07446	4.20E-04	0.05805	0.0018	2.00E-47	1.39E-48
7	1.0745	4.07E-04	0.05832	0.00177	2.14E-47	1.48E-48
6	1.07517	4.13E-04	0.06083	0.00194	2.52E-47	1.96E-48

Table S6. Gaussian fit data of peak 1 of the MPA aerogel.

T / K	x1	Std x1	FWHM1	Std FWHM1	A1	Std A1
295	0.95823	0.00375	0.27703	0.00441	2.83E-47	1.39E-48
270	0.95925	0.00305	0.26976	0.00323	3.44E-47	1.35E-48
240	0.95987	0.00288	0.2457	0.0023	3.64E-47	1.48E-48
210	0.93943	0.00403	0.25118	0.00342	3.37E-47	1.54E-48
180	0.92765	0.00358	0.26634	0.00313	3.37E-47	1.08E-48
150	0.92433	0.00412	2.61E-01	3.75E-03	3.14E-47	1.16E-48
120	0.92889	0.00389	0.25174	0.00352	2.95E-47	1.09E-48
90	0.94138	0.00514	0.22915	0.00428	2.43E-47	1.36E-48
70	0.92603	0.01374	0.19685	0.01465	1.84E-47	3.04E-48
55	0.91669	0.01327	0.20035	0.0152	1.99E-47	3.11E-48
40	0.91789	0.00482	0.27395	0.00522	3.08E-47	1.21E-48
20	0.94863	0.00515	0.2325	0.00388	2.85E-47	1.63E-48
10	0.93676	0.00498	0.24435	0.00437	3.00E-47	1.48E-48
7	0.92511	0.00473	0.25796	0.00486	3.14E-47	1.34E-48
4.2	0.9367	0.00427	0.24407	0.00389	3.24E-47	1.36E-48

Table S7. Gaussian fit data of peak 2 of the MPA aerogel.

T / K	x2	Std x2	FWHM2	Std FWHM2	A2	Std A2
295	1.01666	4.84E-04	0.15887	0.00164	4.38E-47	1.44E-48
270	1.01966	4.06E-04	0.15404	0.00136	5.08E-47	1.38E-48
240	1.01985	4.13E-04	0.14816	0.00136	4.98E-47	1.48E-48
210	1.01878	3.37E-04	0.14646	0.0012	5.55E-47	1.42E-48
180	1.01832	2.84E-04	0.14393	0.001	5.60E-47	1.06E-48
150	1.01952	2.86E-04	0.14167	0.00106	5.37E-47	1.12E-48
120	1.02223	2.75E-04	0.13879	0.00107	4.73E-47	1.04E-48
90	1.02724	3.36E-04	0.13502	0.00145	3.74E-47	1.31E-48
70	1.03153	0.00124	0.13645	0.00216	3.90E-47	2.97E-48
55	1.02776	0.00113	0.13861	0.00186	4.76E-47	3.03E-48
40	1.02489	6.58E-04	0.13441	0.00187	4.22E-47	1.34E-48
20	1.02761	9.31E-04	0.12924	0.00272	3.58E-47	1.89E-48
10	1.02661	6.51E-04	0.13193	0.00206	4.13E-47	1.64E-48
7	1.02587	5.41E-04	0.13379	0.00168	4.51E-47	1.42E-48
4.2	1.02775	5.28E-04	0.13076	0.00174	4.33E-47	1.46E-48

Table S8. Gaussian fit data of peak 3 of the MPA aerogel.

T / K	x3	Std x3	FWHM3	Std FWHM3	A3	Std A3
40	1.08519	0.00363	0.04467	0.01416	4.73E-49	2.81E-49
20	1.08804	0.00245	0.04974	0.01114	7.90E-49	3.96E-49
10	1.0868	0.00209	0.04484	0.00848	7.65E-49	2.82E-49
7	1.08386	0.00209	0.04203	0.00778	7.01E-49	2.32E-49
4.2	1.08671	0.00188	0.04118	0.0072	7.12E-49	2.26E-49

Table S9. Gaussian fit data of peak 1 of the MUA aerogel.

T / K	x1	Std x1	FWHM1	Std FWHM1	A1	Std A1
295	1.00035	4.77E-04	0.21601	8.04E-04	1.51E-46	2.27E-48
270	0.98048	9.66E-04	0.24627	0.00116	1.20E-46	2.21E-48
240	0.96535	0.00119	0.24678	9.82E-04	1.39E-46	2.39E-48
210	0.95161	0.00175	0.24069	0.00114	1.50E-46	3.24E-48
180	0.93113	4.35E-03	0.22997	0.00351	1.41E-46	6.87E-48
150	0.93167	0.00362	2.42E-01	2.94E-03	1.58E-46	6.11E-48
120	0.93226	0.00386	0.24469	0.00282	1.61E-46	6.79E-48
90	0.94728	9.08E-04	0.24922	0.0013	2.06E-46	2.20E-48
70	0.94798	8.49E-04	0.24816	0.00122	2.20E-46	2.07E-48
55	0.94615	8.63E-04	0.25115	0.00127	2.28E-46	2.11E-48
40	0.94954	8.06E-04	0.24522	0.00114	2.36E-46	2.05E-48
20	0.94976	7.94E-04	0.24506	0.00111	2.39E-46	2.01E-48
10	0.95028	8.21E-04	0.24517	0.00115	2.48E-46	2.13E-48
7	0.95172	8.03E-04	0.24377	0.00112	2.54E-46	2.16E-48
4.2	0.95107	8.18E-04	0.24324	0.00114	2.76E-46	2.39E-48

Table S10. Gaussian fit data of peak 2 of the MUA aerogel.

T / K	x2	Std x2	FWHM2	Std FWHM2	A2	Std A2
295	1.02802	3.37E-04	0.1345	1.26E-03	6.53E-47	2.28E-48
270	1.02463	2.12E-04	0.14861	7.29E-04	1.34E-46	2.23E-48
240	1.02362	1.80E-04	0.14877	5.97E-04	1.85E-46	2.39E-48
210	1.02353	1.79E-04	0.14891	6.27E-04	2.26E-46	3.20E-48
180	1.02357	1.93E-04	0.15168	8.62E-04	2.70E-46	6.72E-48
150	1.02E+00	3.72E-04	0.15125	1.06E-03	2.68E-46	6.73E-48
120	1.01791	5.38E-04	0.15106	0.00149	2.55E-46	8.01E-48
90	1.00095	1.11E-03	0.12385	0.00182	1.59E-46	4.83E-48
70	0.99597	8.37E-04	0.11611	0.00149	1.44E-46	3.63E-48
55	0.99265	6.37E-04	0.11358	0.00128	1.48E-46	3.13E-48
40	9.90E-01	5.27E-04	1.07E-01	1.11E-03	1.32E-46	2.56E-48
20	0.98762	4.34E-04	0.10235	9.82E-04	1.27E-46	2.21E-48
10	0.98687	3.97E-04	0.10031	9.47E-04	1.30E-46	2.20E-48
7	0.98674	3.80E-04	0.09907	9.23E-04	1.30E-46	2.18E-48
4.2	0.98608	3.63E-04	0.09864	9.11E-04	1.42E-46	2.35E-48

Table S11. Gaussian fit data of peak 3 of the MUA aerogel.

T / K	x3	Std x3	FWHM3	Std FWHM3	A3	Std A3
150	1.07683	8.56E-04	0.06469	0.00343	7.55E-48	9.96E-49
120	1.08183	5.27E-04	0.06969	0.0027	1.40E-47	1.57E-48
90	1.07824	8.94E-04	0.09041	0.00125	6.44E-47	3.73E-48
70	1.07707	7.21E-04	0.08851	9.81E-04	7.59E-47	2.82E-48
55	1.07724	5.93E-04	0.08601	8.81E-04	7.83E-47	2.28E-48
40	1.07616	5.20E-04	0.08486	8.20E-04	8.18E-47	1.91E-48
20	1.07594	4.44E-04	0.08316	7.64E-04	8.34E-47	1.65E-48
10	1.07616	4.18E-04	0.08164	7.61E-04	8.55E-47	1.62E-48
7	1.07614	4.00E-04	0.081	7.44E-04	8.74E-47	1.60E-48
4.2	1.07595	3.93E-04	0.08025	7.50E-04	9.28E-47	1.70E-48

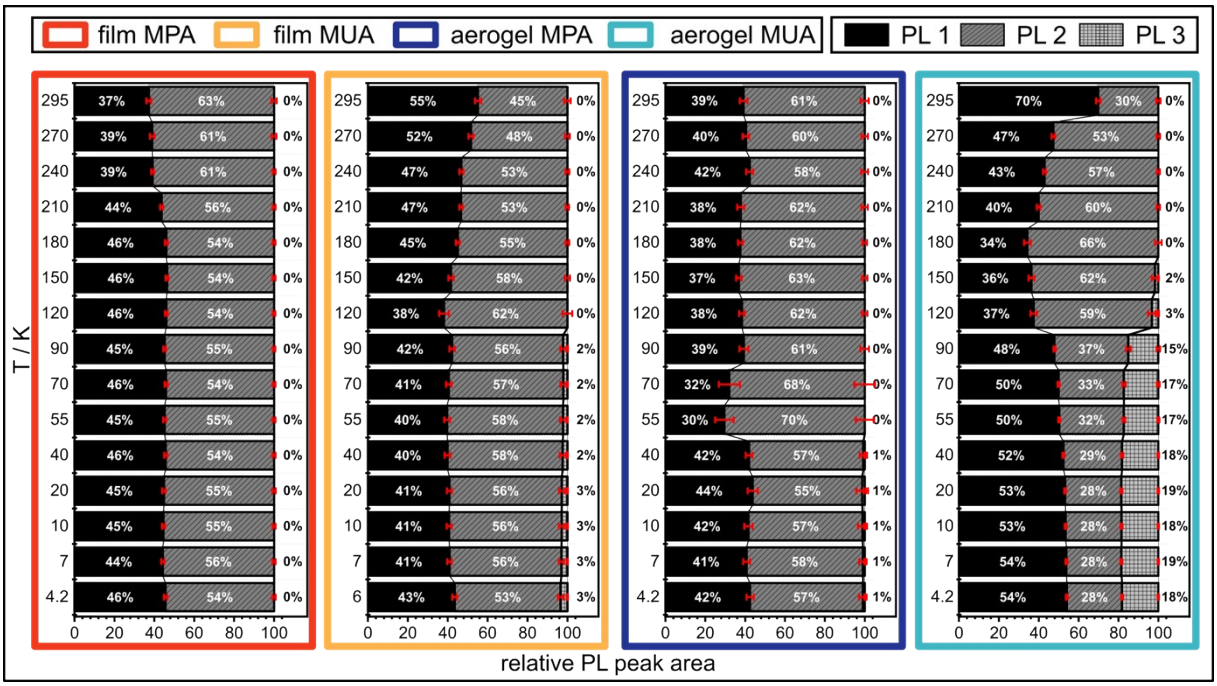

Figure S1. Relative PL peak areas extracted from the Gaussian fit data of the four samples measured at cryogenic temperatures.

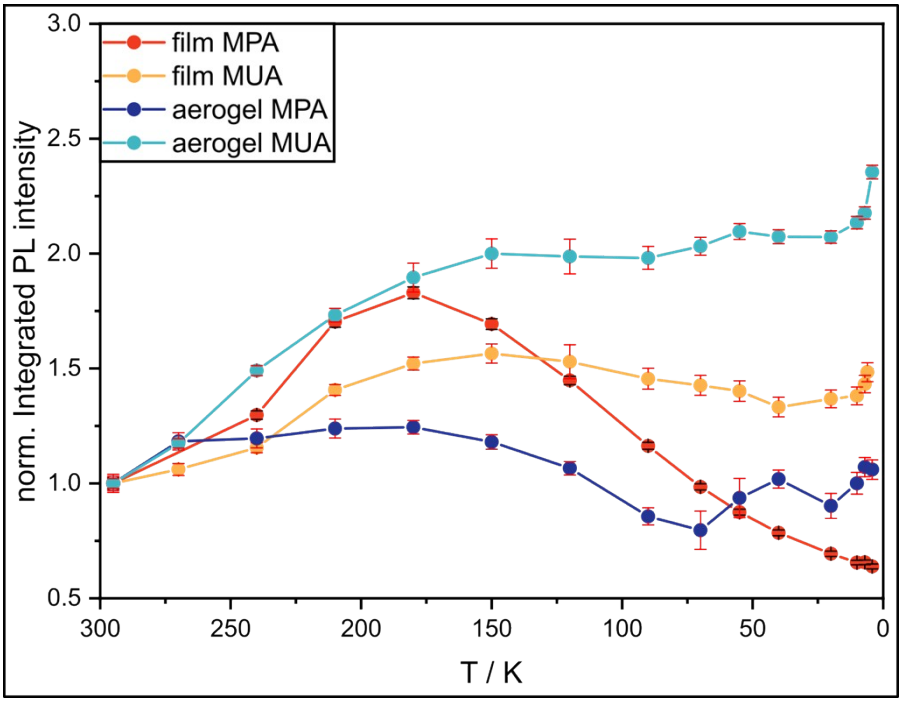

Figure S2. Normalized integrated PL intensities between 4.2 and 295 K, extracted from the Gaussian fit data for the four samples measured at cryogenic temperatures.

Table S12. Calculated average amplitude weighted lifetimes, PLQY and radiative and non-radiative recombination rates of the samples studied. The amplitude weighted lifetimes were calculated from the fit data of the mono- and bi-exponential fits of the PL decays. The number of exponents (# exp.) in the used fits is indicated.

Sample	E_{Em} [eV]	<τ> / ns	PLQY	k_r / ms^{-1}	k_{nr} / ms^{-1}	# exp.
PbS/CdS oleate QD colloid	1.24	2508.5	3.8 %	118.8	279.8	mono
	1.16	2107.1		141.4	333.2	mono
	1.10	2123.2		140.4	330.6	mono
	1.03	2008.1		148.4	349.6	mono
	0.97	1791.0		166.4	392.0	mono
MPA film	1.18	125.9	1.0 %	51.6	5111.8	bi
	1.10	263.2		26.0	2572.0	bi
	1.03	422.2		18.8	1857.2	bi
	0.96	589.1		15.4	1527.9	bi
	0.90	499.1		20.0	1983.7	mono
MUA film	1.21	283.6	2.3 %	34.0	1325.5	bi
	1.13	551.7		25.5	993.8	bi
	1.06	1064.1		16.9	657.5	bi
	0.98	1369.6		16.0	622.1	mono
	0.92	887.2		18.7	729.6	mono
MPA aerogel	1.18	425.3	2.5 %	34.0	1325.5	bi
	1.11	659.1		25.5	993.8	bi
	1.04	1162.1		16.9	657.5	bi
	0.97	1567.3		16.0	622.1	mono
	0.92	1336.3		18.7	729.6	mono
MUA aerogel	1.18	915.7	3.8 %	27.4	694.7	bi
	1.11	1280.9		22.7	574.3	bi
	1.04	2031.5		16.2	410.6	bi
	0.97	2165.8		17.5	444.2	mono
	0.92	1969.9		19.3	488.4	mono

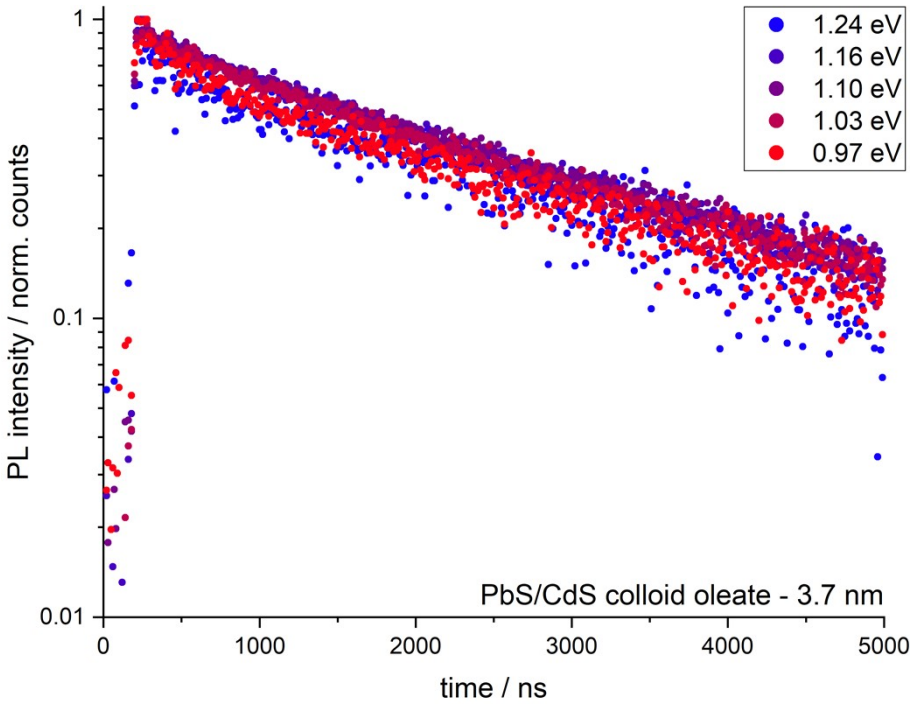

Figure S3. PL decays of the PbS/CdS QD colloid, measured at five positions at the indicated PL energies.

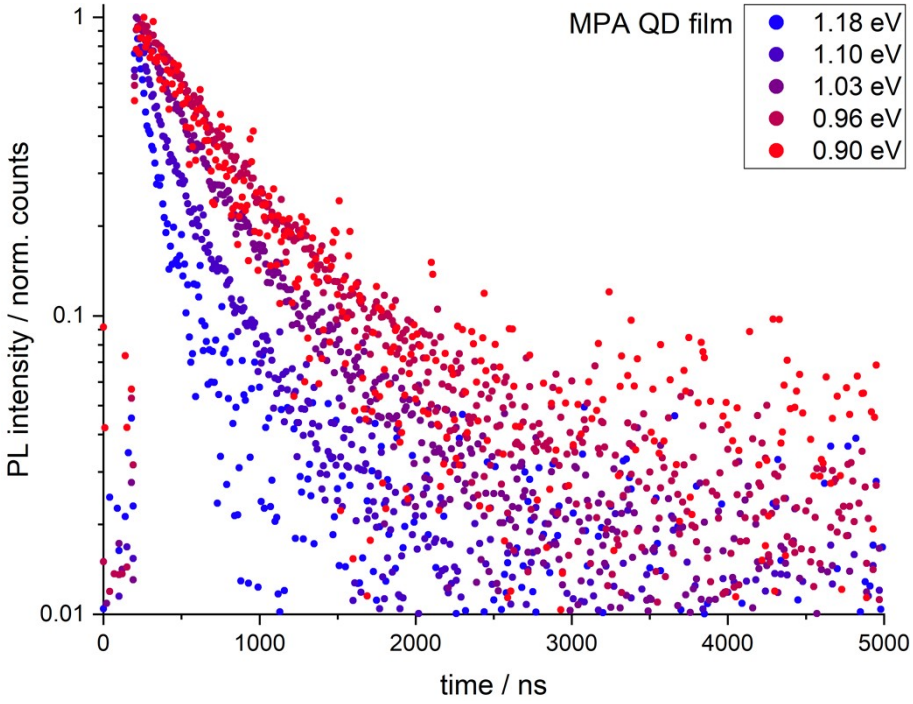

Figure S4. PL decays of the MPA QD film, measured at five positions at the indicated PL energies.

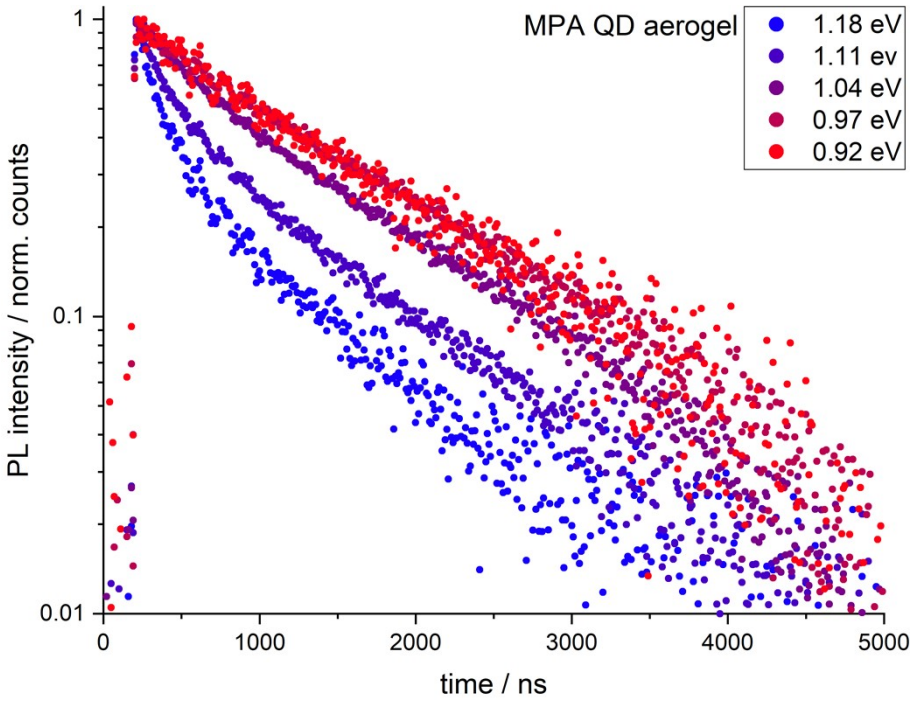

Figure S5. PL decays of the MPA QD aerogel, measured at five positions at the indicated PL energies.

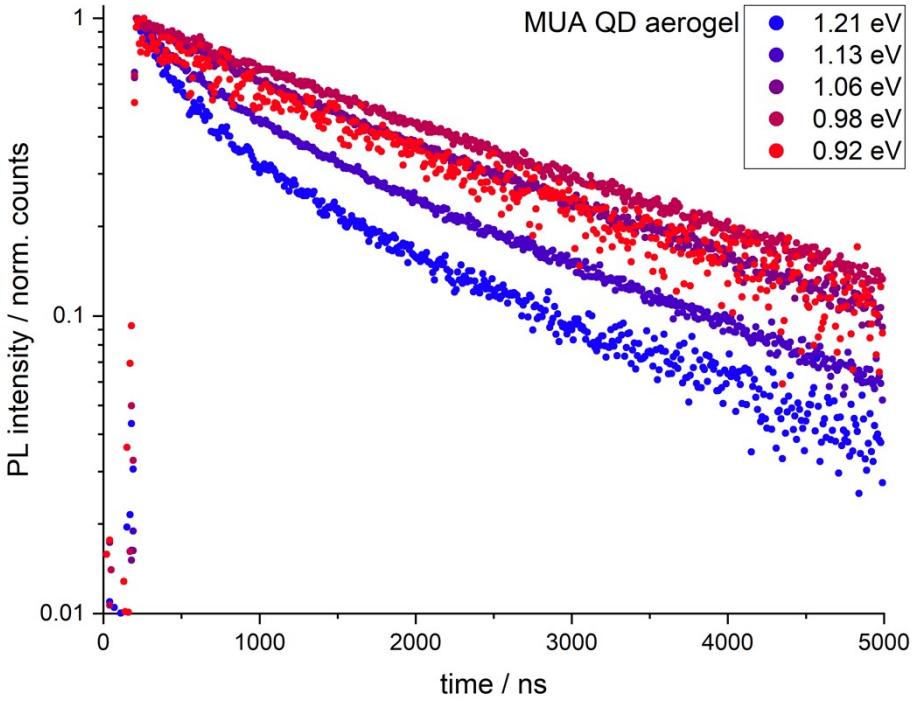

Figure S6. PL decays of the MUA QD aerogel, measured at five positions at the indicated PL energies.

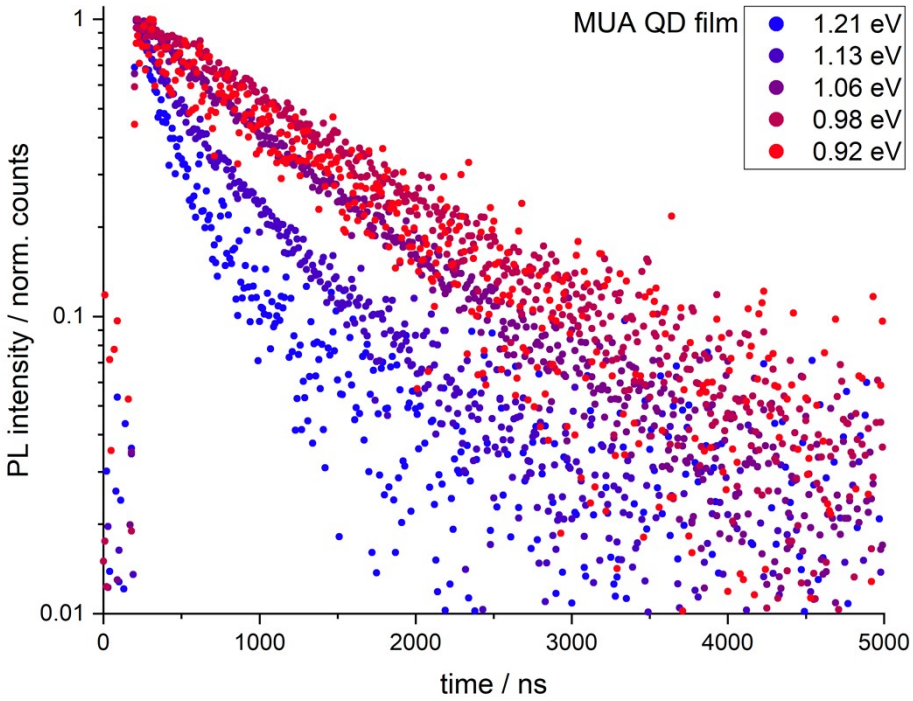

Figure S7. PL decays of the MUA QD film, measured at five positions at the indicated PL energies.

References

[1] J. Zhang, R. W. Crisp, J. Gao, D. M. Kroupa, M. C. Beard, J. M. Luther, *J. Phys. Chem. Lett.* **2015**, *6*, 1830.

[2] H. Zhao, M. Chaker, N. Wu, D. Ma, *J. Mater. Chem.* **2011**, *21*, 8898.

[3] T. Kodanek, H. M. Banbela, S. Naskar, P. Adel, N. C. Bigall, D. Dorfs, *Nanoscale* **2015**, *7*, 19300.

[4] H. G. Bagaria, E. T. Ada, M. Shamsuzzoha, D. E. Nikles, D. T. Johnson, *Langmuir* **2006**, *22*, 7732.

[5] D. Zámbó, A. Schlosser, P. Rusch, F. Lübkemann, J. Koch, H. Pfnür, N. C. Bigall, *Small* **2020**, *16*, DOI: 10.1002/smll.201906934.

[6] D. Pluta, H. Kuper, R. T. Graf, C. Wesemann, P. Rusch, J. A. Becker, N. C. Bigall, *Nanoscale Adv.* **2023**, 5005.

[7] A. Schlosser, L. C. Meyer, F. Lübkemann, J. F. Miethe, N. C. Bigall, *Phys. Chem. Chem. Phys.* **2019**, *21*, 9002.

[8] J. Mooney, P. Kambhampati, *J. Phys. Chem. Lett.* **2013**, *4*, 3316.

[9] C. Li, A. P. Tardajos, D. Wang, D. Choukroun, K. Van Daele, T. Breugelmans, S. Bals, *Ultramicroscopy* **2021**, *221*, 113195.